Hindawi
International Journal of Polymer Science
Volume 2023, Article ID 8407907, 13 pages
https://doi.org/10.1155/2023/8407907

Research Article

The Effect of Resin Matrix on the Properties of CF/PEI and CF/PAEK Thermoplastic Composites

Wencai Wang, Jindong Zhang, Dongting Gao, Kun Yu, Gang Liu, Ming Wang, and Jianan Yao

Center for Advanced Low-Dimension Materials, State Key Laboratory for Modification of Chemical Fibers and Polymer Materials, College of Materials Science and Engineering, Donghua University, Shanghai 201620, China

Correspondence should be addressed to Jianan Yao; yjn@dhu.edu.cn

Received 11 July 2023; Revised 21 August 2023; Accepted 13 September 2023; Published 25 September 2023

Academic Editor: Chenggao Li

As the adhesive for composites, the resin matrix directly impacts the molding process and product performance of thermoplastic composites (TPCs). Carbon fiber-reinforced polyetherimide (CF/PEI) and polyaryletherketone (CF/PAEK) composites were prepared by a compression molding process. The interface, interlaminar, and low-speed impact properties of TPCs were studied. The results show that the interfacial shear strength of the CF/PEI composite is ~116 MPa, while the CF/PAEK composite is ~78 MPa. However, the interlaminar and low-speed impact performance of CF/PAEK is better than CF/PEI. Type I fracture toughness (G_{IC}) and type II fracture toughness (G_{IIC}) of CF/PEI are ~1051 MPa and ~1060 MPa. But those of CF/PAEK are ~1786 MPa and ~2584 MPa, respectively. The compressive strength after the impact of CF/PAEK (~321 MPa) is 40% higher than CF/PEI (~230 MPa).

1. Introduction

Thermoplastic resins can be divided into general-purpose plastics, engineering plastics, and specialist plastics according to their properties and uses. Meanwhile, they can be divided into amorphous and crystalline polymers depending on whether they are crystallized. At present, specialist plastics are used as matrixes for thermoplastic composites (TPCs), mainly including amorphous polymers, polyethersulfone (PES), polyetherimide, semicrystalline polymer polyphenylene sulfide (PPS), and polyetheretherketone (PEEK). TPCs with good impact resistance and damage tolerance have attracted increasing attention in aerospace. In addition, compared to traditional thermosetting composites, TPCs also have the characteristics of recyclability, fast processing, and infinite shelf life of prepreg materials [1–3]. Therefore, TPCs have a broad market application space in the automobile industry, rail transit, transportation, and aerospace [4–7].

PEI is an amorphous thermoplastic polymer with high-temperature resistance, excellent mechanical properties, electrical properties, and dimensional stability. In addition, low melt viscosity endows it with good molding performance. Therefore, PEI received great attention during the development and application of early TPCs. As a member of the most common and widely applied semicrystalline thermoplastic resin, PEEK has been used as a matrix in aeronautical structural composites with good impact resistance, high-temperature resistance, and mechanical properties [8]. However, the harsh molding temperature of close to 400°C makes the process cost higher. Therefore, a low melting temperature has been developed and applied, which changes the regular structure of the main chain compared to that of PEEK. While maintaining PEEK's high-temperature resistance and mechanical properties, the melting temperature of PAEK has been reduced by 30-40°C, which improves its process performance significantly. The molecular structure analysis shows that PEI and PAEK contain rigid functional groups and flexible ether bond structures, such as benzene rings or aromatic imides. The rigid functional groups endow them with high-temperature resistance and excellent mechanical properties, while the ether bond makes them good rheological properties required in the molding process

of TPCs. The difference in the content of ether bonds in the molecular structure shows that PAEK has better toughness than PEI.

Several studies have shown that matrix properties influence the interfacial properties [9–11] and the mechanical properties [12–19] of composites. During the composite failure process, microcracks initially occur in the matrix [20]. When matrix cracks propagate to the interface, two competing fracture failure mechanisms must be considered. On the one hand, if the interface bonding strength is strong enough, the matrix cracks can directly propagate through the fiber, which triggers a brittle failure of composites. On the other hand, if the bonding strength is weak, the crack of the matrix can be deflected along the fiber/matrix interface and continue to propagate along it. The propagation requires energy, which delays structural damage [21]. Therefore, the interfacial properties and the crack propagation resistance of the matrix are important factors affecting the mechanical properties of composites. Gu et al. [14] studied the effect of different viscosity PAEK resins on the interfacial properties of composite materials. The study showed that the interfacial shear strength (IFSS) between low-viscosity resin and fiber was about 23% higher than that of high-viscosity PAEK. The 90° tensile strength of the composite is increased by about 38% by improving the interfacial strength. The research group previously studied the effect of resin crystallinity on the interface properties. The results showed that the lower the crystallinity and smaller the crystals, the better the interface and mechanical properties of the composite materials [15]. Furthermore, the toughness of the resin matrix has an essential influence on the toughness of the fracture and the low-speed impact performance of the composite. [22] found that by improving the toughness of the matrix, the toughness of interlaminar fracture of composite materials can be improved, which is beneficial in preventing crack propagation, delaying the occurrence of delamination, and reducing delamination damage. Kim and Ye [23, 24] studied the effect of resin toughness on the interlaminar fracture toughness of CF/PEI composites. The results show that the fracture toughness for composites with strong interfacial properties is mainly affected by the properties of the matrix. With the improvement of the toughness of PEI resin, the interlaminar fracture toughness of CF/PEI composites has been effectively improved. As far as the author knows, there is relatively little literature on the influence of resin matrix on the properties of thermoplastic composites, and there is even a lack of systematic comparative studies on the properties of different thermoplastic composites.

In this paper, the effect of the crystallization behavior of PEI and PAEK on the interfacial properties of composites was discussed by microdebonding experiments. CF/PEI and CF/PAEK were prepared by compression molding. Meanwhile, the effect of the resin matrix on the interlaminar and low-speed impact properties of TPCs was studied. The study helps to understand the influence mechanism of matrix properties on the interface properties and mechanical properties of TPCs. At the same time, it can provide technical support and references for the design, manufacture, and application selection of TPCs in aviation and aerospace.

Table 1: Mechanical properties of PEI and PAEK.

Type	Test standard	PEI	PAEK
Tensile strength (MPa)	ISO 527	110	96
Tensile modulus (GPa)		3.2	3.8
Flexural strength (MPa)	ISO 178	160	151
Flexural modulus (GPa)		3.3	3.6
Charpy impact, notched ($kJ \cdot m^{-2}$)	ISO 179/1eA	4.0	6.5

2. Materials and Methods

2.1. Raw Materials. The amorphous polymer PEI is provided by SABIC Company (ULTEM™ 1000F3SP, Saudi Arabia) and the semicrystalline polymer PAEK by Tangyuanxian Hairuite Engineering Plastics Co., Ltd. (PAEK-L, China). The mechanical properties of the two kinds of TPs are shown in Table 1. Figure 1 shows the molecular structure formulas of PEI and PAEK. The PEI molecular chain with aromatic imine ring structure is more rigid than PAEK with a benzene ring and low ether bond content (the mass fraction of oxygen in PEI ether bonds is about 5.41%, and the mass fraction of ether bond oxygen in PAEK is about 8.74-11.07%). The difference in structure makes PAEK resin have higher toughness and extensibility. The T700 grade CF is provided by Weihai Expand Fiber Co., Ltd. (TZ700S-12K, China).

CF/PEI and CF/PAEK thermoplastic prepregs were provided by Heilongjiang Yingchuang New Materials Co., Ltd. (TZ700S/PEI and TZ700S/PAEK-L, China), the areal density of the fiber is 149 g/m^2, and the matrix content is 37 wt%. The nominal layer thickness of prepreg is 0.13 mm.

2.2. Preparation of Composites. The preparation of TPCs is shown in Figure 2. First, the prepreg was cut and stacked with a size of 320 mm*260 mm. Second, the preform was produced by ultrasonic spot welding (KH-2870Z, Kehai, China). Third, the welded preform was placed in a die, and the welded preform was placed in a mold and heated by a hot press (HS100/1-400/400, Hengsheng, China). The die was heated according to the molding process. The molding process of CF/PEI composite is 300 ∘ C/0.5 MPa/30 min + 340 ∘ C/1 MPa/30 min, and that of CF/PAEK is 300 ∘ C/0.5 MPa/30 min + 360 ∘ C/2 MPa/30 min, as shown in Figure 3. Finally, the pressure would be maintained until demolding below 100°C at a cooling rate of 1°C/min. The stacking sequence of test specimens is different. The 90° tensile is $[0]_{16}$, the short beam shear is $[0]_{40}$, the G_{IC} and G_{IIC} are $[0]_{24,}$ and the low-speed impact is $[(45/0/-45/90)]_{4S}$. The thickness of test specimens is 2 mm, 5 mm, 3 mm, and 4 mm, respectively. The internal quality of the composites was tested by metallographic microscopy and ultrasonic C-scanning, as shown in Figure 4. The typical scan parameters (transmission mode; ultrasonic frequency, 30 MHz; and signal gain, 28 dB) were carried out.

2.3. Crystallization Behavior Tests. A differential scanning calorimeter (DSC 250, TA, USA) conducted the thermal behavior tests. Under nitrogen protection, the sample weighing 3-10 mg was used for testing with a flow rate of 50 ml/min. First, the sample was heated to 400°C at a heating rate

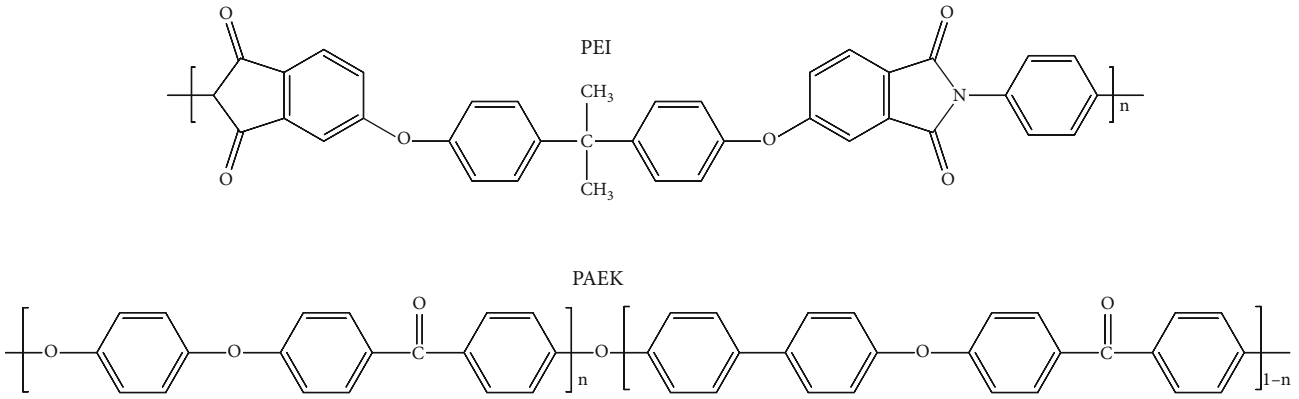

Figure 1: The molecular structures of PEI and PAEK.

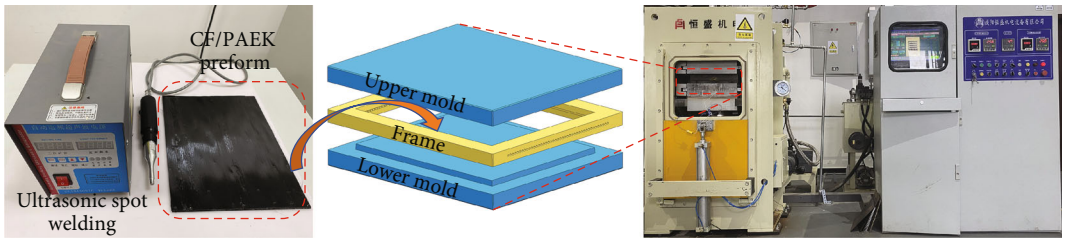

Figure 2: Preparation of thermoplastic composites.

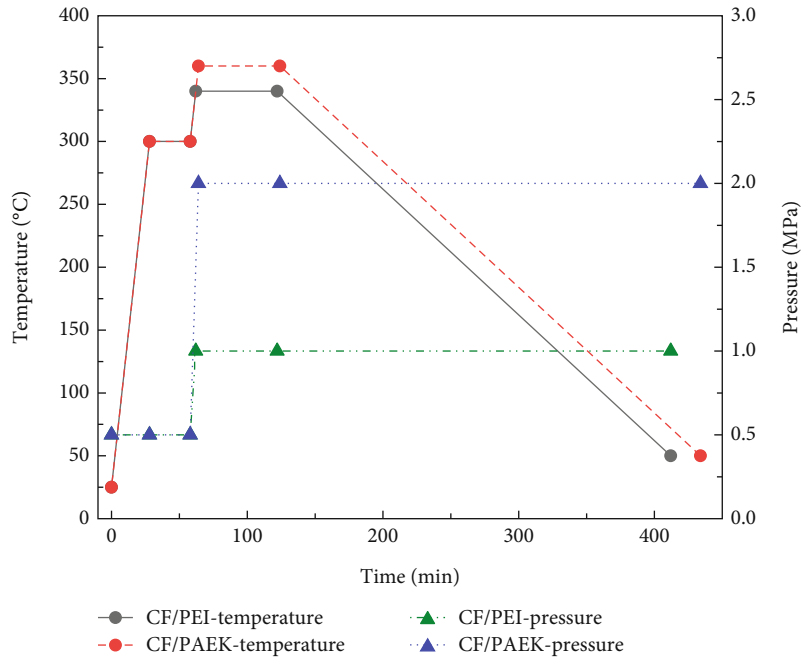

Figure 3: Molding process diagram of thermoplastic composites.

of 20°C/min and then kept for 5 minutes to erase thermal history. Second, they were cooled to 50°C at 1°C/min cooling rates. Finally, the sample was reheated to 400°C.

The crystallization behaviors of the polymers were observed by a polarizing microscope (DM4 P, Leica, Germany) equipped with a polarizer. First, a single CF was fixed on a hot stage, and the resin powder was evenly spread on the surface of the CF. Second, the polymer was heated to 360°C and kept for 5 minutes to ensure complete melt. Finally, the sample was cooled to 30°C at a rate of 1°C/min, and the crystallization morphology of the polymer on the fiber surface could be observed in real time.

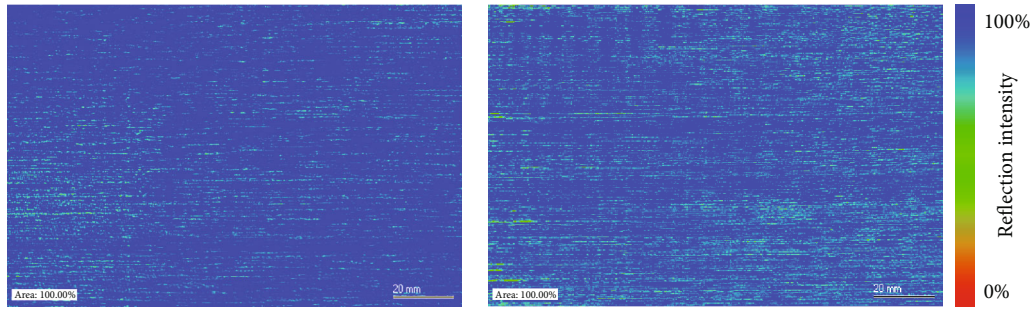

(a) (b)

Figure 4: Internal quality of thermoplastic composites: (a) CF/PEI and (b) CF/PAEK.

2.4. Interface Property Tests. IFSS between fiber and resin was tested by a composite interface performance evaluation device (HM410, Tohei Sangyo, Japan). First, the monofilament separated from the fiber bundle was fixed on a concave metal fixture. Second, the metal fixture was installed in the furnace, where the temperature was increased to 380°C (PEI) and 350°C (PAEK) to melt the thermoplastics. The thermoplastics formed several elliptical microspheres on the surface of the carbon fiber due to surface tension. Finally, the sample was cooled to room temperature at 1°C/min. Precise force transducers record the tensile load during the test. IFSS is calculated by [14]

$$\tau = \frac{F}{\pi DL}, \tag{1}$$

where τ is the IFSS, F is the maximum tensile load, D is the fiber diameter, and L is the embedded fiber length.

2.5. Mechanical Property Tests. All laminates of TPCs were prepared by a water-jet machine (OMAX, ProtoMAX, USA) and tested by a universal testing machine (5982-100kN, Instron, USA).

The 90° tensile properties were tested using ASTM D 3039. The specimen size is 175 mm × 25 mm × 2 mm (length × width × thickness), and sandpaper is used at both ends of the clamping.

The short beam shear properties were tested according to ASTM D 2344. The specimen size is 30 mm × 10 mm × 5 mm, and the span-to-measured thickness ratio is 4.0.

The interlaminar fracture toughness tests referred to ASTM D 5528 and ASTM D 7905. The specimen size is 180 mm × 25 mm × 3 mm. The prefabricated crack length is 50 mm for G_{IC}, and that of G_{IIC} is 40 mm. The G_{IC} was measured using the double cantilever beam (DCB) test and the compliance calibration (CC) method. The numerical calculation is shown in

$$G_{IC} = \frac{nP\delta}{2ab}, \tag{2}$$

where n is the CC coefficient, which is the slope of the lg (δ_i/P_i) fit line versus lg (a_i) plot using the visually observed delamination onset values and all the propagation values, P is the maximum force, δ is the load point displacement, a is the delamination length, and b is the specimen width. The support span for the G_{IIC} testing is 100 mm, and that of G_{IIC} can be calculated using

$$G_{IIC} = \frac{3mP^2a^2}{2B}, \tag{3}$$

where m is the CC coefficient, P is the maximum force, a is the crack length used in the fracture test, and B is the specimen width.

The low-speed impact properties of composites were tested using a floor-standing impact system (CEAST 9350, Instron, USA) based on ASTM D 7136. The drop hammer weighed 10.28 kg with a 16 mm diameter impacter, and the impact energy was set at 6.67 J/mm. The nominal size of the specimen is 150 mm × 100 mm × 4 mm. Compression strength after impact (CAI) performance tests was completed by a 600 kN universal mechanical testing machine (E45.605, MTS, USA) referring to ASTM D 713. The torque of the screws is 7 N·m, and the speed of the compressive testing is 1.25 mm/min.

2.6. Microscopic Morphology Analysis. The scanning electron microscope (Regulus SU8230, Hitachi, Japan) was used to observe the microscopic morphology of failed specimens and analyze the difference between CF/PEI and CF/PAEK. Before that, the exciting specimens were dried at 120°C for 4 h in a hot air circulation oven and then pretreated with gold spray for 60 s. The accelerating voltage is set at 10 kV.

3. Results and Discussion

3.1. Internal Quality of Thermoplastic Composites. Whether the matrix resin can impregnate the reinforcing fibers well will directly affect the final product's performance for fiber-reinforced composites, so ensuring the internal quality of the composites is a prerequisite. Ultrasonic C-scanning is a relatively common test method for detecting the internal quality of composites. It can be seen from Figure 4 that the CF/PEI and CF/PAEK appear blue overall, and there is no obvious difference in distribution, indicating that the

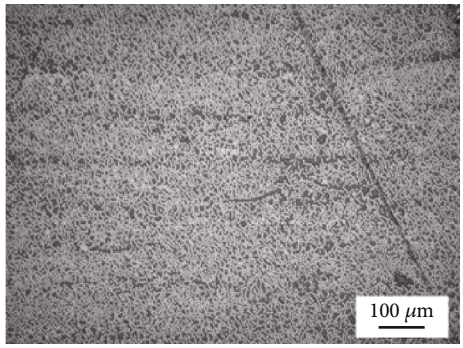

Figure 5: Microscopic morphology of the CF/PEI composite.

internal quality is similar and good. At the same time, obvious void defects were not found by observing the morphology of the composites, as shown in Figure 5.

3.2. Crystallization Behavior of Resins. The thermal properties and crystallization behaviors of the polymers are shown in Figure 6. A comparison of curves indicates an obvious difference in thermal properties. In Figure 6(a), PEI exhibits the typical thermal behavior of amorphous polymers, while in Figure 6(b), PAEK exhibits the typical thermal behavior of semicrystalline polymers. PAEK has two characteristic peaks during the first heating process. The first characteristic peak is the cold crystallization peak, and the second characteristic peak is the melting peak. The sharp crystallization peak represents the phase-transition process of PAEK in the amorphous region. There is no cold crystallization distinct peak in PAEK during the second heating process. Therefore, PAEK can be nearly fully crystallized at a 1°C/min cooling rate, and the crystallinity is approximately 33.8%. The crystallinity (X_c) of the resin can be calculated by

$$X_c = \frac{\Delta H_c}{\Delta H_f^0} \times 100\%, \quad (4)$$

where ΔH_c is the melting enthalpy of the DSC test and ΔH_f^0 is the theoretic melting enthalpy of completely crystallized PAEK taken as 130 J/g [25].

It can be seen from Figure 7(a) that there is no crystalline structure inside the PEI, but as shown in Figure 7(b), a large amount of spherulites is generated inside the PAEK.

3.3. The Effect of Resin on the Interfacial Properties of Composites. Plots of IFSS stress versus displacement are shown in Figure 8. IFSS of CF/PEI is 115.6 ± 11.9 MPa, and that of CF/PAEK is 78.2 ± 7.0 MPa. Compared to the IFSS data of CF/PEI and CF/PAEK, the interfacial bonding strength of CF/PEI is higher than that of CF/PAEK under the same cooling conditions. The surface morphology after microdebonding experiments can help explain the phenomenon, as shown in Figure 9. It can be seen in Figure 9(a) that the surface of PEI resin is smooth with no apparent shrinkage phenomenon. However, the PAEK is rough and covered with different sizes of pits, as in Figure 9(b). PAEK with a specific dense spherulite structure is almost completely crystallized at a cooling rate of 1°C/min. This will generate internal stress at the interface between the matrix and CF due to solidification shrinkage. This mechanism can be better understood in Figure 10. However, some experimental studies have shown that, for some fiber systems, the transcrystalline structures on the fiber's surface are conducive to improving the interface bonding strength. For example, Chen and Hsiao [26] studied the transcrystalline structure of various single-filament systems. The results showed that the IFSS had greater than 40% increases with transcrystalline designs compared to the system without transcrystalline facilities. It should be noted that the transcrystalline structures of PAEK are not found around the CF in this experiment, as shown in Figure 7(b).

Plots of 90° tensile strength versus strain are shown in Figure 11. 90° tensile strength and modulus of CF/PEI are 46.9 ± 3.2 MPa and 8.5 ± 0.9 GPa, while those of CF/PAEK are 42.3 ± 2.0 MPa and 11.2 ± 1.1 GPa. 90° tensile strength of CF/PEI is higher but has a lower modulus, which is consistent with the properties of the resin matrix. The failure morphology of the composites after testing is shown in Figure 12. The surface of the fibers is completely covered with resin, indicating that the failure of composites occurs in the resin layer. Therefore, both composites have good interfacial bonding strength, even stronger than the matrix. Furthermore, it can be found that the section morphology of the composites is quite different. The PEI has a relatively smooth surface, while the surface of PAEK is covered with dense hackle structures. This phenomenon is related to the property of the plastic deformation capacity of the resin.

3.4. Effect of the Matrix on Interlaminar Properties of Composites. The interlaminar shear strength (ILSS) of CF/PAEK (90.5 ± 0.5 MPa) is higher than that of CF/PEI (86.7 ± 1.2 MPa). Figure 13 shows the typical plots of ILSS stress versus displacement, which shows that the CF/PEI has no apparent yield behavior, and the failure occurs instantaneously when the loading displacement reaches about 0.9 mm. In contrast, the stress of the CF/PAEK drops slowly after reaching its peak and then up and down multiple cycles. This difference in failure mode has a great relationship with the plastic deformation capacity of the matrix under a stronger interface strength. It can be seen from Table 1 that PAEK resin has better-notched impact toughness than PEI. The PEI is more brittle than PAEK, and cracks are easier to gather and produce larger through cracks. However, the PAEK with better plastic deformation capacity can reduce stress concentration and form many microcracks, which can absorb more energy with increased strain. Figure 14 can further explain this phenomenon. However, Gu et al. [14] believe that the interlaminar shear properties of thermoplastic composites are affected by the interfacial properties, and composites with stronger interfaces have higher ILSS. Still, it cannot explain our experimental results. Therefore, the ILSS of composites can be affected by both resin matrix and interfacial properties.

The G_{IC} of CF/PAEK (1786 ± 72 MPa) is higher than that of CF/PEI (1051 ± 76 MPa). At the same time, the G_{IIC}

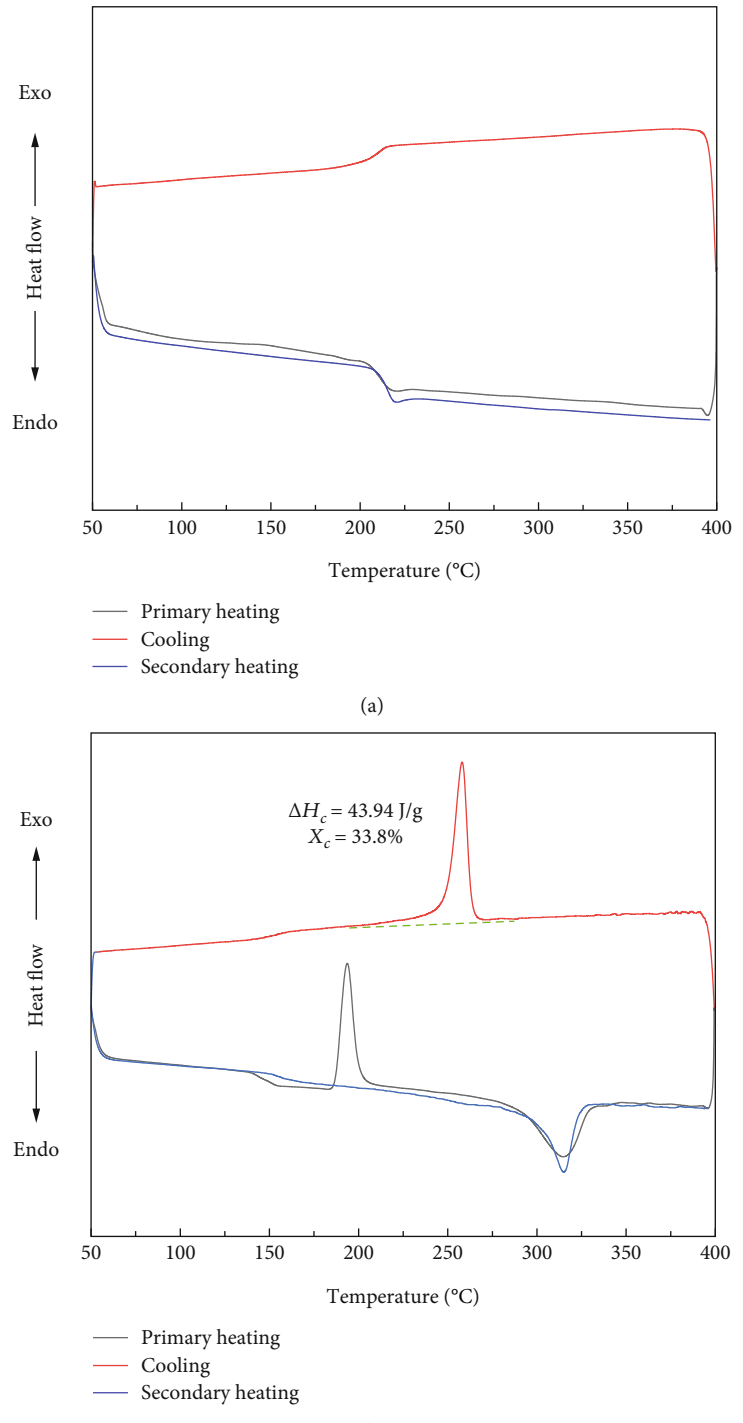

Figure 6: Thermal performance characterization results of (a) PEI and (b) PAEK.

of CF/PAEK (2584 ± 168 MPa) is higher than that of CF/PEI (1060 ± 119 MPa). Therefore, CF/PAEK has better interlaminar fracture toughness, mainly due to the greater plastic deformation capacity of PAEK resin. Figures 15(a) and 15(b) show the failure morphologies of the G_{IC} samples. After the failure of the test, the resin layer of the CF/PEI type I specimen is relatively smooth. On the other hand, the CF/PAEK composite cross-section has a rough resin appearance, which is conducive to the resin's absorption of external energy during the test [15]. The fracture morphology of the type II sample is shown in Figures 15(c) and 15(d). The failure morphology of the resin matrix of the two composite materials is tear-like. It has the same orientation behavior as the stress mode (shear force) of the composites. The difference is that the tear size of the PAEK resin is relatively large. It can be found that a dense thermoplastic resin layer

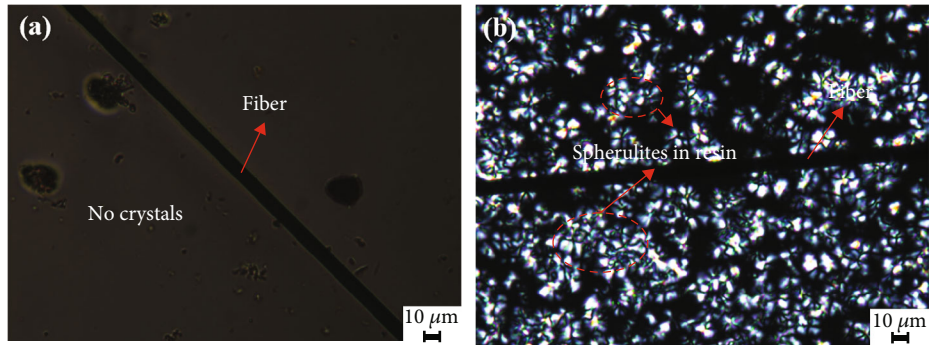

Figure 7: Aggregated morphology of (a) CF/PEI and (b) CF/PAEK.

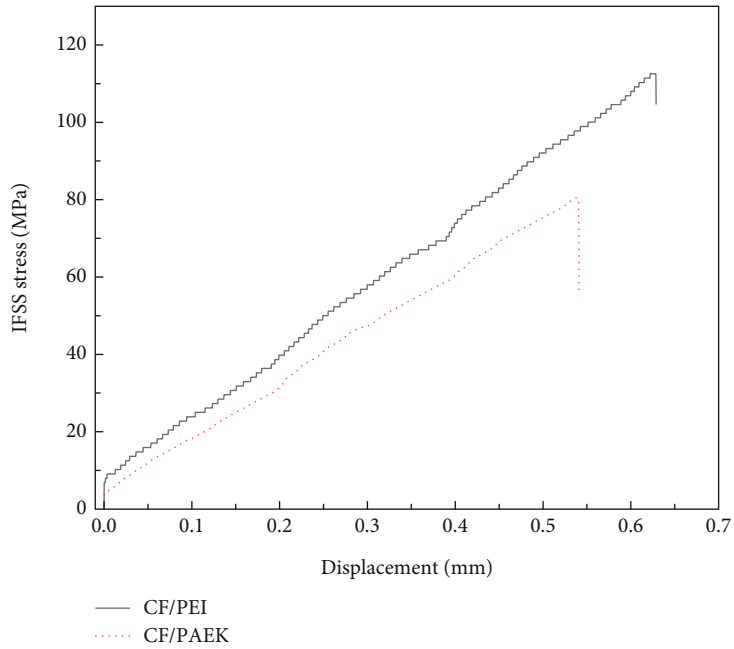

Figure 8: Typical IFSS stress-displacement curves of CF/PEI and CF/PAEK composites.

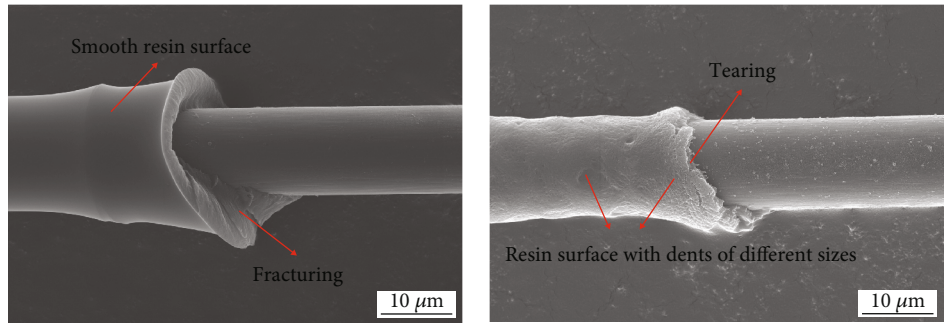

(a) (b)

Figure 9: Surface morphology after microsphere debonding of composites: (a) CF/PEI and (b) CF/PAEK.

is attached to the fracture surfaces of the two composites, and the fibers are completely wrapped by the resin, which indicates that the interface is not damaged during the interlayer slip of the composites. Gao and Kim [27] considered the interlaminar fracture toughness of composites to be a complex interaction of two basic properties, the plastic deformation capacity of the matrix and the bond strength of the fiber-matrix interface. Therefore, for composites with

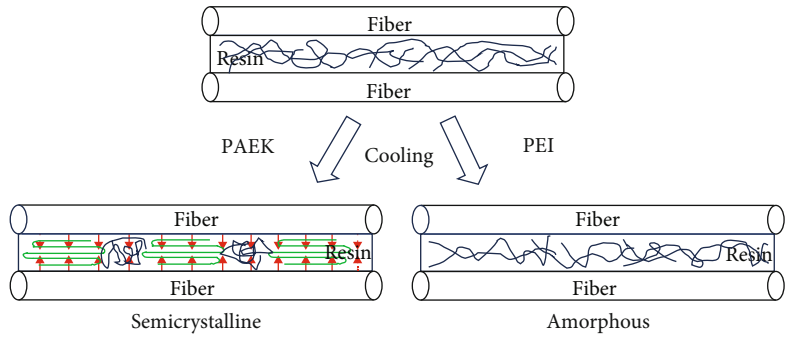

Figure 10: Mechanism diagram of the aggregate structure change of the two resins.

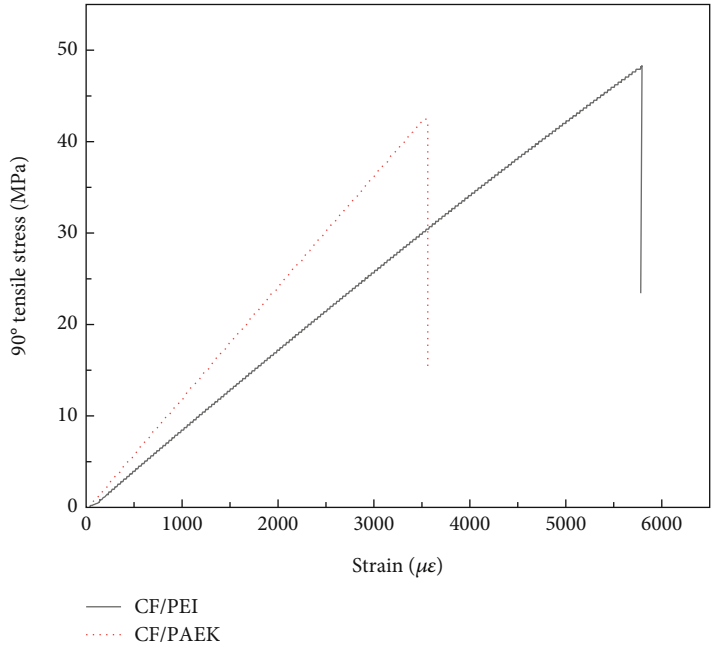

Figure 11: Typical 90° tensile stress-strain curves of CF/PEI and CF/PAEK composites.

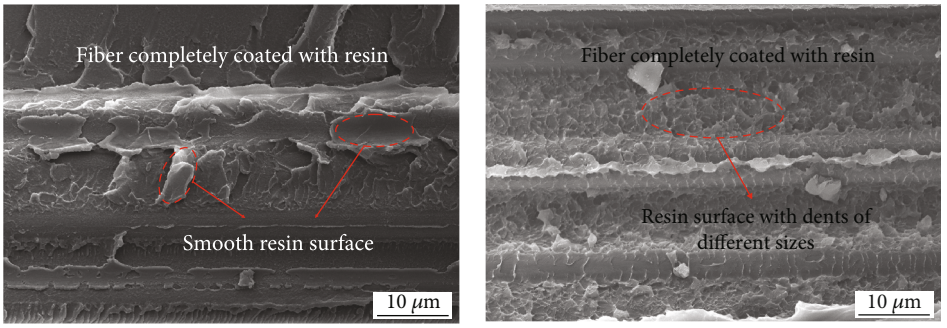

(a) (b)

Figure 12: 90° tensile fracture morphology of (a) CF/PEI and (b) CF/PAEK.

strong interfacial strength, the plastic deformation capacity of the resin matrix determines the interlaminar fracture toughness. The resin's force pattern during the test can be better understood in Figure 16.

3.5. Effect of Resin on the Low-Speed Impact Properties of Composites. Typical impact load-displacement and energy-time curves of CF/PEI and CF/PAEK are shown in Figure 17. The energy losses of CF/PEI and CF/PAEK are

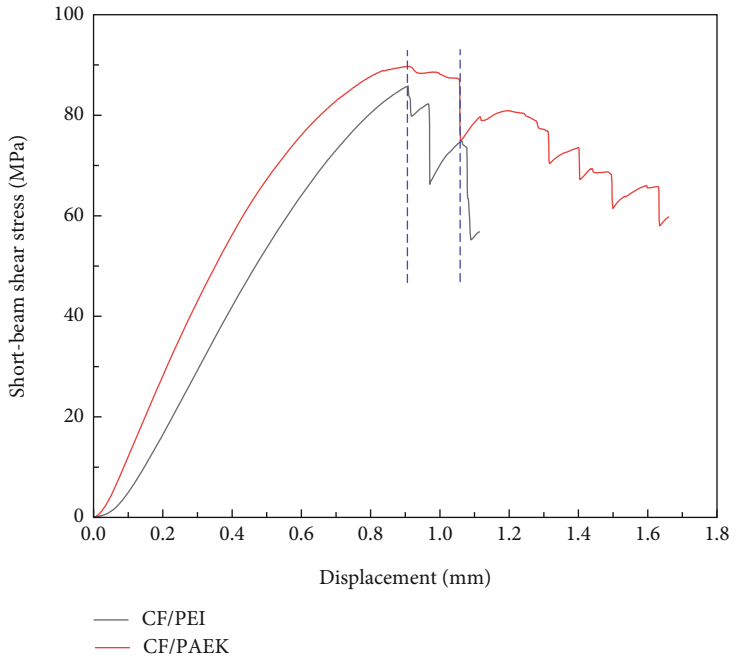

Figure 13: Typical short beam shear stress-displacement curve of CF/PEI and CF/PAEK composites.

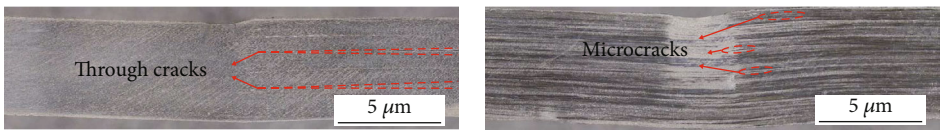

(a) (b)

Figure 14: Cross-sectional morphology of (a) CF/PEI and (b) CF/PAEK after short beam tests.

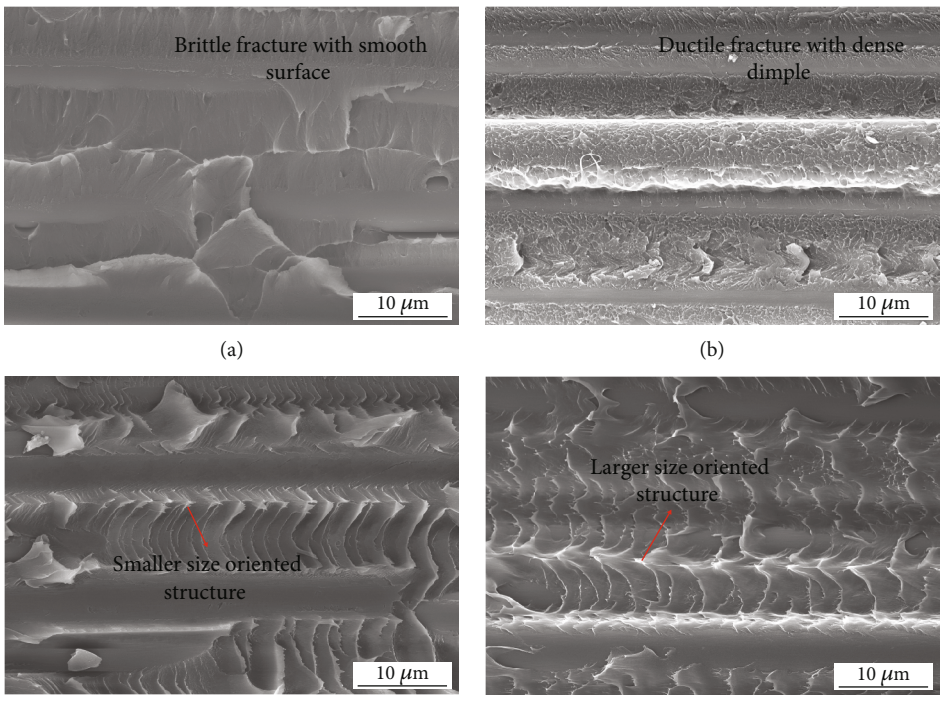

(a) (b) (c) (d)

Figure 15: Fracture morphology of composites: (a) G_{IC} of CF/PEI, (b) G_{IC} of CF/PAEK, (c) G_{IIC} of CF/PEI, and (d) G_{IIC} of CF/PAEK.

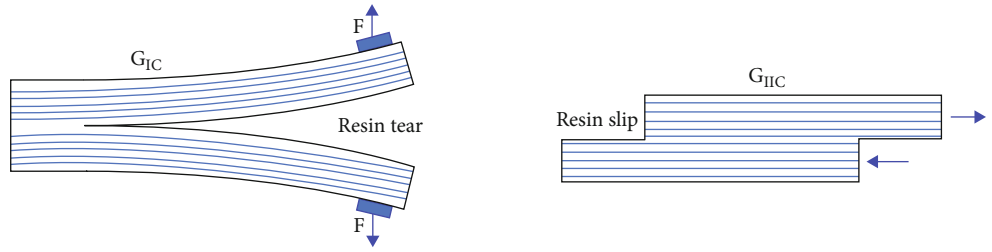

Figure 16: Schematic diagram of G_{IC} and G_{IIC} testing for composites.

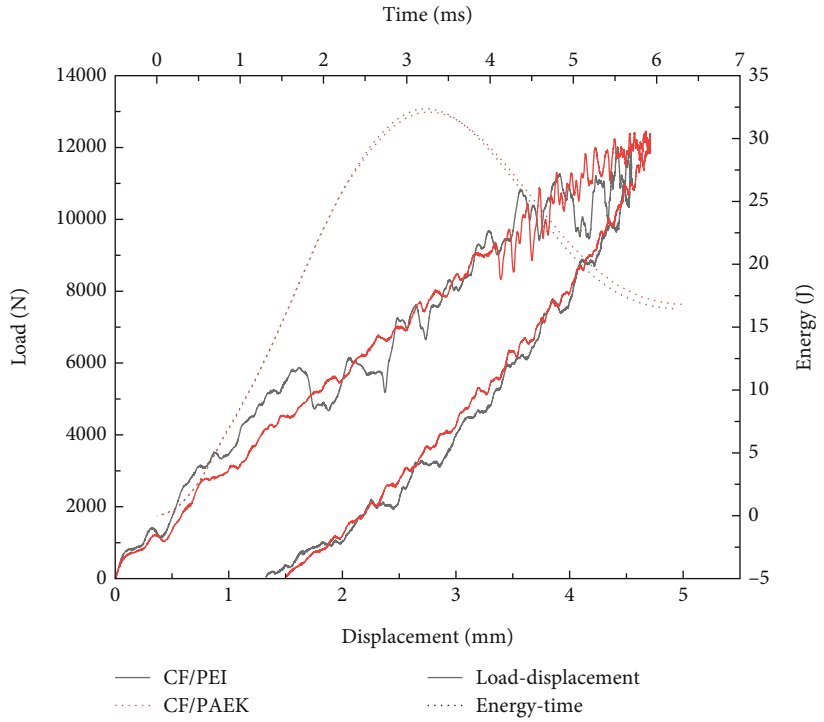

Figure 17: Typical impact load-displacement and energy-time curves of CF/PEI and CF/PAEK composites.

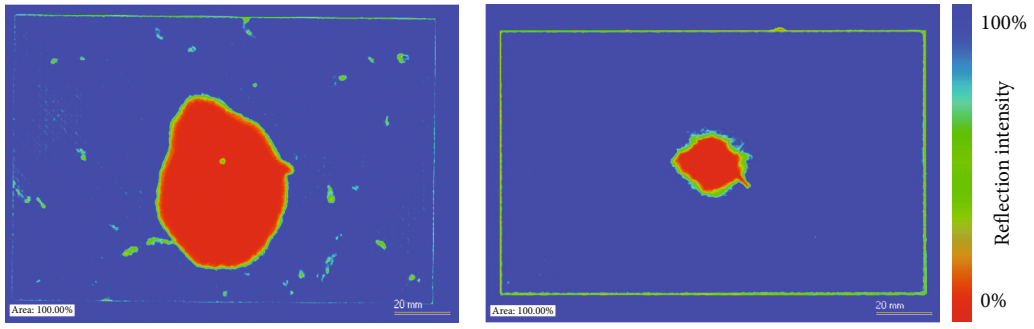

(a) (b)

Figure 18: The projection area of the impact damage sites: (a) CF/PEI and (b) CF/PAEK.

15.83 ± 0.37 J and 15.45 ± 1.69 J, respectively, indicating that the absorption of impact energy by the composites is almost the same. More dense and volatile zigzags exist on the load-displacement curves of CF/PEI. These zigzags correspond to cracks and delamination.

The impact damage mechanisms in laminates constitute a complex process resulting from a combined interaction of matrix cracking, delamination, fiber shear, and fiber breakage [28, 29]. The indentation depth of CF/PEI (0.30 ± 0.02 mm) is about 20% lower than that of CF/PAEK (0.36 ± 0.02 mm). The specific impact damage projection area of the composites for ultrasonic C-scan testing is shown in Figure 18. The damaged area of the CF/PEI composite is 26.82 ± 1.55 cm^2, and that of the CF/PAEK composite is

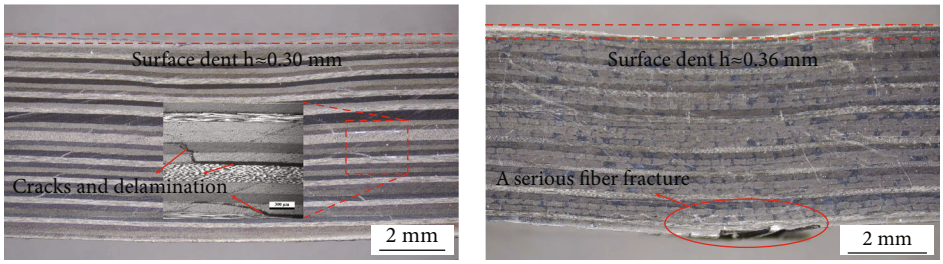

(a) (b)

Figure 19: The cross-sectional images of the impact damage sites: (a) CF/PEI and (b) CF/PAEK.

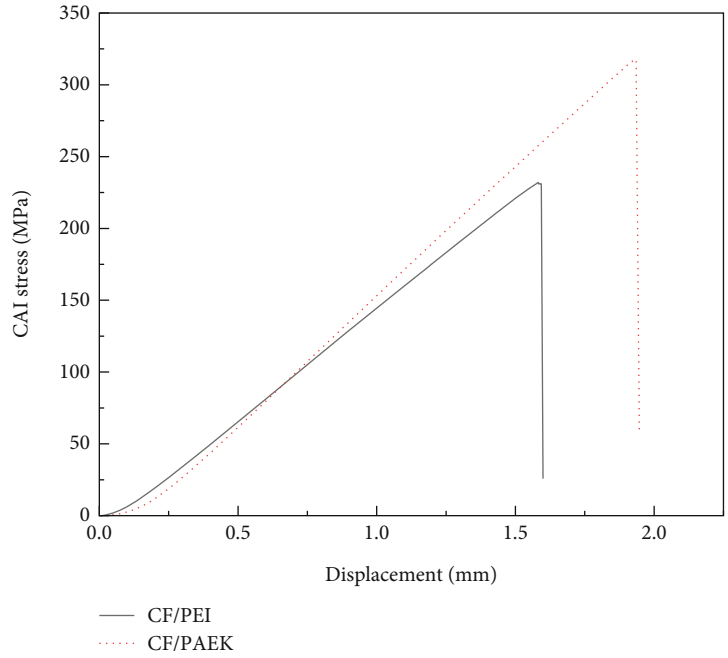

Figure 20: Typical CAI stress-displacement curves of CF/PEI and CF/PAEK composites.

$4.19 \pm 0.18\,cm^2$. The damaged area is about 540% higher than the latter, indicating a difference in the damage mechanism between the CF/PEI and CF/PAEK. The differences between damage patterns can be identified with cross-sectional views (see Figure 19). Obvious delamination and fiber breakage occurred after CF/PEI impact failure. In contrast, the fibers on the back of CF/PAEK were severely broken, and there was no obvious delamination between layers. Zhang et al. [15] used XRM to reconstruct 3D samples of TPCs after impact, and the results showed that the composite with higher G_{IIC} mainly absorbed energy through the plastic deformation of the resin matrix. Instead, they absorb energy primarily through layering. The interlaminar fracture toughness data in the previous section show that CF/PAEK has higher G_{IIC} than CF/PEI composite, and PAEK resin has better plastic deformation ability. Therefore, the CF/PAEK composite mainly absorbs energy through the plastic deformation ability of the resin to reduce interlayer damage. However, the CF/PEI composite mainly absorbs impact energy through fiber fracture and layer crack propagation.

Plots of CAI stress versus displacement are shown in Figure 20. The CAI strength of CF/PEI (230 ± 5 MPa) is lower than that of CF/PAEK (321 ± 7 MPa), indicating that the latter maintains high mechanical properties after impact damage. The residual strength is strongly related to the interfacial bond properties and G_{IC} but largely depends on the size of the damaged area after impact [30, 31]. The CF/PAEK has a lower G_{IC} and damaged area than the CF/PEI. Therefore, CF/PAEK composites exhibit higher CAI strength.

4. Conclusions

In this study, CF/PEI and CF/PAEK thermoplastic composites with good quality were successfully prepared by the hot pressing process. At the same time, their interfacial, interlayer, and low-speed impact properties were comparatively studied. CF/PEI has better interfacial properties than CF/PAEK, which may be related to the crystallization difference of the resin during the cooling process because the volume shrinkage of the PAEK resin during the crystallization

process produces stress. When the stress is transmitted to the interface, the bond strength between the fiber and the resin is weakened. On the contrary, the interlayer performance of CF/PAEK composites is significantly better than that of CF/PEI. The G_{IC} and G_{IIC} of the CF/PAEK are about 70% and 144% higher than those of the CF/PEI. This is mainly affected by the toughness of the resin matrix. The impact of PAEK's better plastic deformation ability can absorb more energy to resist the damage of the resin matrix. Also affected by the deformation ability of the resin, the low-speed impact failure mechanisms of the two composites are different. CF/PEI composites mainly absorb energy from fiber failure and ply crack propagation. CF/PAEK composites mainly absorb energy through the plastic deformation ability of resin to reduce impact damage and exhibit higher compressive strength after impact. The CAI strengths of CF/PEI and CF/PAEK composites are 230 MPa and 321 MPa, respectively.

Data Availability

All data are included within the article.

Conflicts of Interest

The authors declare that they have no conflicts of interest.

Acknowledgments

Thanks are due to Dr. Lei Liu and Dr. Mengyao Zhang for their help with the measurement and characterization. The authors are grateful for the financial support from the Fundamental Research Funds for the Central Universities (no. 2232022A-12).

References

[1] B. A. Alshammari, M. S. Alsuhybani, A. M. Almushaikeh et al., "Comprehensive review of the properties and modifications of carbon fiber-reinforced thermoplastic composites," *Polymers*, vol. 13, no. 15, p. 2474, 2021.

[2] M. Yilmaz, N. F. Yilmaz, and M. F. Kalkan, "Rheology, crystallinity, and mechanical investigation of interlayer adhesion strength by thermal annealing of polyetherimide (pei/ultem 1010) parts produced by 3d printing," *Journal of Materials Engineering and Performance*, vol. 31, no. 12, pp. 9900–9909, 2022.

[3] X. Gabrion, V. Placet, F. Trivaudey, and L. Boubakar, "About the thermomechanical behaviour of a carbon fibre reinforced high-temperature thermoplastic composite," *Composites Part B: Engineering*, vol. 95, no. 1, pp. 386–394, 2016.

[4] K. Friedrich, A. D. Amore, D. Acierno, and L. Grassia, "Carbon fiber reinforced thermoplastic composites for future automotive applications," *AIP Conference Proceedings*, vol. 1736, article 020001, 2016.

[5] V. Uday, S. L. Jin, and M. G. Jia, "Thermoplastic composites for aerospace applications," *Aeronautical Manufacturing Technology*, vol. 483, no. 14, pp. 69–71, 2015.

[6] Y. F. Luo and N. Y. Jia, "Applications of high-performance thermoplastic composites in civil aviation," *Aeronautical Manufacturing Technology*, vol. 64, no. 16, pp. 93–102, 2021.

[7] Y. Wan and J. Takahashi, "Development of carbon fiber-reinforced thermoplastics for mass-produced automotive applications in japan," *Journal of Composites Science*, vol. 5, no. 3, p. 86, 2021.

[8] J. Q. Hu, B. Wang, H. Q. Zhang, and K. L. An, "Preparation of thermoplastic composite components and their applications in aerospace," *Astronautical Systems Engineering Technology*, vol. 4, no. 4, pp. 61–70, 2020.

[9] S. Huo, A. Thapa, and C. A. Ulven, "Effect of surface treatments on interfacial properties of flax fiber-reinforced composites," *Advanced Composite Materials*, vol. 22, no. 2, pp. 109–121, 2013.

[10] S. Kantharaju, J. Vinodhini, M. Govindaraju, and S. Bhowmik, "An investigation to enhance the mechanical property of high-performance thermoplastic composite through different plasma treatment," *Polymer Composites*, vol. 44, no. 1, pp. 178–189, 2023.

[11] P. F. Li, J. Z. Zhou, L. L. Li et al., "Influence of depositing sequence and materials on interfacial characteristics and mechanical properties of laminated composites," *Materials Science and Engineering A*, vol. 827, no. 1, article 142092, 2021.

[12] R. R. Ma, X. Z. Zhou, Y. Wang, and W. Zhang, "Effect of the toughness of resin matrix on mechanical properties of composites," *Acta Aeronautica Et Astronautica Sinica*, vol. 8, no. 2, pp. 94–102, 1983.

[13] L. N. Tian, *Study on Forming Process and Mechanical Properties of Carbon Fiber Reinforced Thermoplastic Resin-Based Composite Material*, Changchun University of Technology, ChangChun, China, 2012.

[14] Y. Y. Gu, J. N. Yao, L. F. Wang, G. Liu, C. H. Chen, and S. G. Yang, "Influence of poly aryl ether ketone resin matrix properties on interfacial properties and interlayer properties of composites," *Acta Materiae Compositae Sinica*, vol. 40, no. 8, pp. 4481–4490, 2023.

[15] J. D. Zhang, G. Liu, P. An et al., "The effect of cooling rates on crystallization and low-velocity impact behaviour of carbon fibre reinforced poly(aryl ether ketone) composites," *Composites Part B: Engineering*, vol. 254, no. 1, article 110569, 2023.

[16] Y. Y. Gu, J. Zhang, G. Liu, Y. T. Liu, J. Gan, and S. G. Yang, "Effect of melt viscosity and impact energy of poly aryl ether ketone(PAEK) resins on the impact damage behavior of their composites," *Acta Materiae Compositae Sinica*, vol. 40, no. 10, pp. 5017–5029, 2023.

[17] W. I. Lee, M. F. Talbott, G. S. Springer, and L. A. Berglund, "Effects of cooling rate on the crystallinity and mechanical properties of thermoplastic composites," *Journal of Reinforced Plastics and Composites*, vol. 6, no. 1, pp. 2–12, 1987.

[18] Y. Ma, Y. Yang, T. Sugahara, and H. Hamada, "A study on the failure behavior and mechanical properties of unidirectional fiber reinforced thermosetting and thermoplastic composites," *Composites Part B: Engineering*, vol. 99, no. 1, pp. 162–172, 2016.

[19] W. Woigk, C. A. Fuentes, J. Rion et al., "Interface properties and their effect on the mechanical performance of flax fibre thermoplastic composites," *Composites Part A: Applied Science and Manufacturing*, vol. 122, no. 1, pp. 8–17, 2019.

[20] S. Huang, Q. Fu, L. Yan, and B. Kasal, "Characterization of interfacial properties between fibre and polymer matrix in composite materials – a critical review," *Journal of Materials Research and Technology*, vol. 13, no. 1, pp. 1441–1484, 2021.

[21] Z. M. Zhu, Z. R. Yang, and H. Jiang, "Review of interfacial debonding behavior of adhesive structures with soft materials," *Chinese Journal of Theoretical and Applied Mechanics*, vol. 53, no. 7, pp. 1807–1828, 2021.

[22] R. M. Wang and R. R. Ma, "The effect of matrix toughness on the damage resistance of composite orthogonal laminated plates," *Composites Science and Engineering*, vol. 15, no. 4, pp. 1–5, 1988.

[23] K. Kim and L. Ye, "Interlaminar fracture toughness of cf/pei composites at elevated temperatures: roles of matrix toughness and fibre/matrix adhesion," *Composites Part A: Applied Science and Manufacturing*, vol. 35, no. 4, pp. 477–487, 2004.

[24] K. Kim, L. Ye, and C. Yan, "Fracture behavior of polyetherimide (pei) and interlaminar fracture of cf/pei laminates at elevated temperatures," *Polymer Composites*, vol. 26, no. 1, pp. 20–28, 2005.

[25] J. N. Panda, J. Bijwe, and R. K. Pandey, "Optimization of the amount of short glass fibers for superior wear performance of PAEK composites," *Composites Part A: Applied Science and Manufacturing*, vol. 116, pp. 158–168, 2019.

[26] E. J. H. Chen and B. S. Hsiao, "The effects of transcrystalline interphase in advanced polymer composites," *Polymer Engineering and Science*, vol. 32, no. 4, pp. 280–286, 1992.

[27] S. Gao and J. Kim, "Cooling rate influences in carbon fibre/peek composites. Part ii: interlaminar fracture toughness," *Composites Part A: Applied Science and Manufacturing*, vol. 32, no. 6, pp. 763–774, 2001.

[28] N. Dubary, C. Bouvet, S. Rivallant, and L. Ratsifandrihana, "Damage tolerance of an impacted composite laminate," *Composite Structures*, vol. 206, no. 1, pp. 261–271, 2018.

[29] T. Shyr and Y. Pan, "Impact resistance and damage characteristics of composite laminates," *Composite Structures*, vol. 62, no. 2, pp. 193–203, 2003.

[30] M. Freitas and L. Reis, "Failure mechanisms on composite specimens subjected to compression after impact," *Composite Structures*, vol. 42, no. 4, pp. 365–373, 1998.

[31] H. Tuo, Z. Lu, X. Ma, J. Xing, and C. Zhang, "Damage and failure mechanism of thin composite laminates under low-velocity impact and compression-after-impact loading conditions," *Composites. Part B, Engineering*, vol. 163, pp. 642–654, 2019.